Physics Letters A ••• (••••) •••–•••

Contents lists available at ScienceDirect

Physics Letters A

www.elsevier.com/locate/pla

Reconfigurable topological phononic crystal slabs

Lu-yang Feng, Hong-bo Huang, Jian-cheng Zhang, Xiao-ping Xie *, Jiu-jiu Chen *

State Key Laboratory of Advanced Design and Manufacturing for Vehicle Body, College of Mechanical and Vehicle Engineering, Hunan University, Changsha 410082, China

ARTICLE INFO

Article history:
Received 27 February 2018
Received in revised form 7 June 2018
Accepted 16 June 2018
Available online xxxx
Communicated by R. Wu

Keywords:
Topological edge state
Reconfigurability
Lamb wave
Pseudospin–orbit coupling
Robustness

ABSTRACT

We propose two-dimensional reconfigurable phononic crystal slabs that support topologically protected edge states for Lamb waves. It consists of a triangular lattice of triangular-like air holes perforated in a slab and two sandwich cylinders are placed in the matrix of each unit cell. The pseudospin–orbit coupling is achieved by shifting the sandwich cylinders up or down. The robust transport of Lamb waves along reconfigurable interfaces is further demonstrated. The dynamically reconfigurable design provides an excellent platform for tuning the frequency range of topological edge states and steering efficient transport of Lamb waves along arbitrary pathways, which can be employed for elastic-wave communications, signal processing, and sensing.

1. Introduction

The discoveries of the quantum Hall effect, the quantum spin Hall effect, and topological insulators have revolutionized our scientific cognition of condensed matter physics. Since the gapless edge states in graphene and HgTe quantum wells were discovered [1,2], more studies on analogous states in structures supporting classical waves have been conducted. Topologically protected edge states have been demonstrated in the topological photonic crystals [3–13], which is of great importance in both fundamental science and the practical application.

In parallel, these concepts have also inspired a novel field of topological acoustics [14–27]. Achieving topologically protected acoustic-wave propagation depends mainly on three categories of mechanisms. The first is to realize one-way edge states similar to the quantum Hall effect. By introducing a circulating fluid flow to break the time-reversal symmetry [14–16], the topologically protected unidirectional edge states with strong robustness were demonstrated in nonreciprocal systems. The second mechanism exhibits the pairwise topological edge states in analogy with the quantum spin Hall effect. By constructing a pair of pseudospins [19–22], the robust pseudospin-dependent transport has been successfully demonstrated in systems with pseudo-time-reversal symmetry. The third is to achieve valley-polarized topological edge states by emulating the valley Hall effect. The topological valley transport has been successfully observed by breaking the spatial-reversal symmetry [23–26]. Different from the previous studies on acoustics in the fluid domain where acoustic waves are purely longitudinal, the research of topological physics in the solid slabs is extremely challenging due to the mixture of all three polarizations of elastic waves. Recently, topologically protected edge states for Lamb waves have been achieved by using a dual-scale topological phononic crystal (TPC) [19]. However, its topological bandgaps and transport pathways are limited to specific situations that cannot be tuned after machining. Most recently, many studies on the reconfigurability of the TPCs have been performed in the fluid domain due to the merits of tuning the topological bandgaps and transport pathways [22,23], which can enrich the design and use of the TPCs. So far, there is few investigation on the reconfigurability of the TPCs in the solid domain owing to the limitation of the movement of the scatterers. Thus, it is meaningful and challenging to investigate the reconfigurable TPCs in the solid domain.

The purpose of this letter is to realize the reconfigurable phononic crystal (PC) slabs supporting topological edge states for Lamb waves. It consists of a triangular lattice of triangular-like air holes perforated in a slab and two sandwich cylinders are inserted in the matrix material of each unit cell. The inversion symmetry breaking caused by moving the sandwich cylinders up or down leads to the pseudospin–orbit coupling. We explicitly demonstrate that the topologically protected transport of Lamb waves is robust against various kinds of defects along reconfigurable interfaces. The tunability of the designed TPC slabs makes it possible to dynamically control the frequency range of topological edge states and

* Corresponding authors.
E-mail addresses: xp_xie@hnu.edu.cn (X.-p. Xie), chen99nju@gmail.com (J.-j. Chen).

https://doi.org/10.1016/j.physleta.2018.06.029
0375-9601/© 2018 Published by Elsevier B.V.

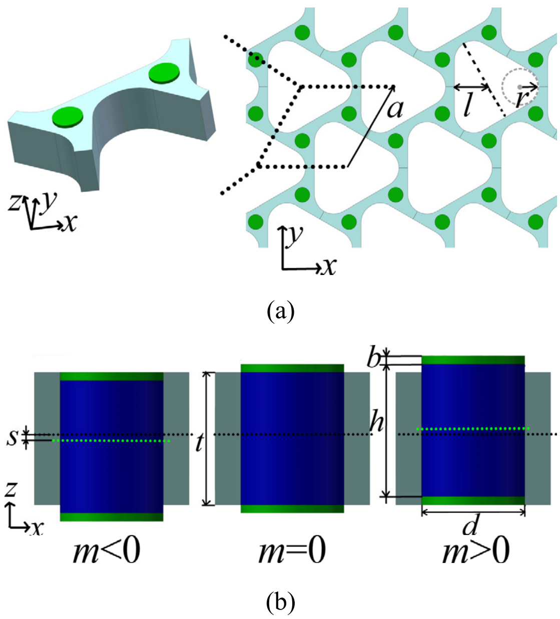

Fig. 1. (a) Perspective view (left panel) of a unit cell and top view (right panel) of the PC slabs formed by a triangular array of triangular-like air holes in a slab. The host material of each unit cell is inserted by two movable sandwich cylinders. (b) Sandwich cylinders at different positions in the slab: from left to right, the sandwich cylinders are shifted from the lower to upper position, leading to a topological transition as indicated by the mass term m. The sandwich cylinder consists of one cylindrical core (blue) in the center and two cylindrical face sheets (green) on both ends. The black and green dotted lines represent the position of the neutral planes of the slab and the sandwich cylinders, respectively. (For interpretation of the colors in the figure(s), the reader is referred to the web version of this article.)

reconfigure arbitrary transport pathways for Lamb waves without obvious backscattering.

2. Reconfigurable topological design

As shown in Figs. 1(a) and (b), the designed PC slabs are composed of a triangular array of triangular-like air holes perforated in an elastic slab and the host material of each unit cell is inserted by two movable sandwich cylinders, each of which consists of one cylindrical core (blue) in the center and two cylindrical face sheets (green) on both ends. The lattice constant is $a = 40$ mm and the slab thickness is $t = 10.5$ mm. The fillet radius of the triangular-like hole is $r = 8.3$ mm and the distance from center to side of the triangular-like hole is $l = 14.85$ mm. The diameter of the cylinder, the length of the cylindrical core, and the thickness of the cylindrical face sheet are $d = 6.4$ mm, $h = 10.5$ mm, and $b = 0.64$ mm, respectively; the displacement of the cylinders is denoted as s (suppose that $s = 0$ mm when the neutral plane of the sandwich cylinders overlaps with that of the slab [middle panel in Fig. 1(b)]). The material of the cylindrical core of the sandwich cylinder is polyetheretherketone (PEEK) which is a common engineering plastics with excellent friction and wear properties as well as mechanical properties, and the material of the remaining structures is steel. The material parameters are chosen as follows: the density $\rho = 7800$ kg/m^3, the Young modulus $E = 206$ GPa, and the Poisson's ratio $\sigma = 0.3$ for steel; $\rho = 1285$ kg/m^3, $E = 4.21$ GPa, and $\sigma = 0.388$ for PEEK. The propagation of Lamb waves is governed by the wave equilibrium equation $\rho\ddot{u} = \nabla(\lambda + 2\mu)(\nabla \cdot u) - \nabla \times (\mu\nabla \times u)$, where ρ is the material density, u is the displacement vector, and both $\lambda = E\sigma/[(1+\sigma)(1-2\sigma)]$ and $\mu = E/[2(1+\sigma)]$ are the Lame's coefficients. The wave equilibrium equation can be transferred into the eigenvalue problem $(\mathbf{K} - \omega^2(k)\mathbf{M})\mathbf{U} = 0$ [28], where $\mathbf{K}$ and $\mathbf{M}$ are the stiffness matrix and mass matrix, respectively, and k represents the wave vector in the irreducible Brillouin zone. The eigenvalue problem is solved by using eigenfrequency analysis of solid mechanics in the commercial finite element software COMSOL Multiphysics. Periodic boundary conditions are imposed on the four external cross section of the unit cell, and the stress-free boundary conditions are set on the other surfaces. When the wave vector k varies along the boundary of the irreducible Brillouin zone (Γ–K(K′)–M–Γ) [inset of Fig. 2(a)], the Lamb-wave band structures $\omega(k)$ are obtained, as shown in Fig. 1(a), (c), and (d).

For a phononic system, it is necessary to increase the degrees of freedom to two-fold states to emulate two pseudospin states [20,22]. Consequently, a four-fold Dirac degeneracy in the phononic band structure is required. For $s = 0$ mm [middle panel of Fig. 1(b)], both the in-plane C_{3v} and the z-direction symmetries of the PC slabs are maintained, resulting in the four-fold Dirac degeneracy at point K [Fig. 2(a)]. The degenerate Lamb-wave modes are classified by their displacement fields as the symmetric (S) modes (blue lines) and the anti-symmetric (A) modes (red lines). The frequency and group velocity of these two families of modes are matched around the Dirac point, which allows one to use unitary transform of the orthogonal basis (S and A modes) as pseudospin states [19,20].

We then introduce pseudospin–orbit coupling to induce topological phase translation, accomplished by the opening of a complete topological bandgap. When the sandwich cylinders are moved up or down from the equilibrium position [left or right panel of Fig. 1(b)], the z-direction inversion symmetry of the PC slabs is broken, leading to the formation of a complete topological bandgap and two two-fold degeneracies: the lower (upper) A and upper (lower) S modes [Fig. 2(c)]. For all frequencies in the proximity of the original Dirac points where the frequency and group velocity degeneracy are maintained, the A and S modes of the PC slabs become hybridized $(A \pm S)/\sqrt{2}$ [19], which can be used as two pseudospin states [20]. As shown in Fig. 2(b), the evolution of displacement fields of the unit cells from $s = 0$ mm to $s \neq 0$ mm also confirms the pairwise hybridizations of the A and S modes. In practice, the z-direction symmetry breaking caused by moving the sandwich cylinders produces an effect analogous to spin–orbit coupling in graphene. To reveal the pseudospin–orbit effect, the effective Hamiltonian for the present PC slabs can be obtained by the perturbation theory as [10,19]:

$$\hat{H} = v_D(\hat{\tau}_z\hat{s}_0\hat{\sigma}_x\delta k_x + \hat{\tau}_0\hat{s}_0\hat{\sigma}_y\delta k_y) + m\hat{\tau}_z\hat{s}_z\hat{\sigma}_z, \tag{1}$$

where $\hat{\sigma}_i$, $\hat{\tau}_i$, and $\hat{s}_i$ ($i = x, y, z$) are the Pauli matrices acting on orbit, valley, and pseudospin state vectors, respectively; $\hat{\tau}_0$ and $\hat{s}_0$ are the identity matrix, v_D is the group velocity near the Dirac point, and m ($|m| = \Delta\omega_{gap}/2$, where $\Delta\omega_{gap}$ is the topological bandgap) is the effective mass induced by the z-direction symmetry breaking. The last term $m\hat{\tau}_z\hat{s}_z\hat{\sigma}_z$ [Eq. (1)] caused by the z-direction symmetry breaking is identical to the spin–orbit coupling of the Kane–Mele Hamiltonian [1], which demonstrates that the z-direction symmetry breaking leads to the pseudospin–orbit coupling in the present PC slabs. The occurrence of the pseudospin–orbit coupling can induce a topological phase transition. In order to reveal the topological phase transition [29,30], the pseudospin Chern numbers are introduced to characterize various topological phases. For the Hamiltonian given in Eq. (1), the pseudospin Chern numbers of each band can be evaluated as $C = \pm sgn(m)$ [10,19]. For $s = 0$ mm [middle panel of Fig. 1(b)], the pseudospin Chern numbers C are equal to zero due to $m = 0$, meaning trivial topological phase; while for $s \neq 0$ mm, the pseudospin Chern numbers C are nonzero due to $m \neq 0$, corresponding to the nontrivial topological phase. Obviously, by moving the sandwich cylinders up or down, the PC slabs experience a topological phase transition. Note

Please cite this article in press as: L.-y. Feng et al., Reconfigurable topological phononic crystal slabs, Phys. Lett. A (2018), https://doi.org/10.1016/j.physleta.2018.06.029